Improved red color with cholesteric liquid crystals in Bragg reflection mode

Peter Kipfer
Institut de Microtechnique
Rue Breguet 2
CH-2000 Neuchâtel
Switzerland

Rolf Klappert
ASULAB SA
Rue des Sors 3
CH-2074 Marin
Switzerland

Hans Peter Herzig
Institut de Microtechnique
Rue Breguet 2
CH-2000 Neuchâtel
Switzerland
E-mail: hanspeter.herzig@unine.ch

Joachim Grupp
ASULAB SA
Rue des Sors 3
CH-2074 Marin
Switzerland

René Dändliker, MEMBER SPIE
Institut de Microtechnique
Rue Breguet 2
CH-2000 Neuchâtel
Switzerland

Abstract. The helical pitch of the cholesteric liquid crystal (CLC) can be adjusted to reflect the colors red, green, and blue. Additive mixing of these colors in displays results in multicolor images and it is easy to use pure primary blue and green colors, but the red color is in general very unsaturated. We show by simulations that this poor red color performance is due to reflection sidebands on the smaller wavelength side of the normal red Bragg reflection band. We discuss five approaches to improve the red color performance, namely, two types of spectral filtering (dyes or filters), a very low birefringence CLC, a gradient in the birefringence of the CLC, and the use of a bluish reflector. The two methods of spectral filtering are also experimentally tested. © *2002 Society of Photo-Optical Instrumentation Engineers.* [DOI: 10.1117/1.1447229]

Subject terms: liquid crystals; cholesteric texture; color generation.

1 Introduction

A lot of research is currently being done on reflective multicolor LCDs for application in personal digital assistants (PDAs), information tools (ITs), or palm tops. There are several different approaches to achieving reflective multicolor LCDs. Supertwisted nematic (STN) LCs in birefringent mode,[1] guest host systems with color filters,[2] and hybrid aligned nematic (HAN) with color filters[3] have been studied among others. Recent work has shown that polymer-stabilized or polymer-free cholesteric texture (PSCT and PFCT) LCDs can be used[4,5] to create multicolor direct-view LCDs. The advantage of cholesteric texture LCDs (CTLCDs) is that they do not require polarizers or reflectors and they offer gray-scale capability and have memory. Additive mixing of primary colors can be done by stacking layers or by juxtaposing differently colored pixels.[6] Unfortunately, it is not possible to obtain saturated red colors with cholesteric LCs (CLCs) without any additional means such as for example dyes.[7] In this paper, we analyze why the red color has poor quality and we discuss five possibilities to overcome the problem. Two of them are based on spectral filtering with dyes or filters and another one uses a blue reflector behind the CLC layer. We also study the influence of a gradient birefringence throughout the CLC layer and a CLC with relatively small birefringence. The methods based on spectral filtering are tested in experiments.

2 CLCs and Their Optical Properties

LC molecules in the cholesteric phase form a helical structure. This structure is periodic along the helical axis (z direction) and the spatial period is given by half the pitch. The pitch p is defined as the distance along z necessary for the molecules to make a complete turn of 2π.

The optical properties of the CLC for light incident parallel to the helical axis depend on the relation between the vacuum wavelength λ_0, the pitch p and the birefringence $\Delta n = n_e - n_o$ of the LC material with n_e and n_o is the extraordinary and ordinary refractive indices, respectively. In our study, only the case of Bragg reflection due to the periodic cholesteric structure is of interest. The condition for Bragg reflection is $\lambda_0 = np$ with $n = (n_e + n_o)/2$. If λ_0 is in the visible range of the spectrum, the CLC appears colored due to the selectively reflected light with the spectral bandwidth of $\Delta\lambda = \Delta np$ and the center wavelength $\lambda_0 = np$. The color of the reflected light depends on the product of np, whereas Δnp determines its saturation and brightness. For nonpolarized light incident parallel to the helical axis, half of it is reflected and half of it is transmitted. The re-

flected and transmitted light are circularly polarized, the handness of the reflected light being the same as that of the cholesteric helix. The transmitted light has the opposite handness. This transmitted light could be reflected by a second CLC layer with the opposite handness to provide nearly 100% reflection for each wavelength in the reflection band. Adding a second CLC layer with the same handness and a $\lambda/2$ wave plate between both layers would give the same result.[8]

3 Brief Description of the Moharam and Gaylord Theory

The exact reflection spectrum can be calculated based on the Moharam and Gaylord theory.[9] The CLC is divided into a large number of uniform birefringent layers perpendicular to the helical axis. The layers are slightly twisted against each other, and their thickness is very small compared with the wavelength of the incident light.

We consider circular polarized light that is incident parallel to the helical axis of the CLC. If the incident circular polarized light is of the same handness as the CLC the light will see a modulation of the effective refractive index n_{eff} given by

$$n_{\text{eff}}(z) = \frac{n_c n_o}{\{[n_o \cos \varphi(z)]^2 + [n_c \sin \varphi(z)]^2\}^{1/2}}, \quad (1)$$

with extraordinary and ordinary indices of refraction n_e and n_o, twist angle of the helix $\varphi(z) = 2\pi z/p$, location along helix axis z, and length of pitch p.

The solution of the Helmholtz equation leads to a superposition of two plane waves. The first is traveling forward, the second backward. The reflected and transmitted amplitudes are obtained by matching the electrical field E and its derivation at the boundaries between the layers and at the boundaries between the LC and the input and output regions.

The Helmholtz equation in a medium with the refraction index n_{eff} is given as

$$(\Delta + n_{\text{eff}}^2 k^2) E = 0, \quad (2)$$

with the Laplacian operator Δ and the wave vector $\mathbf{k} = 2\pi/\lambda$.

A normal incident circular polarized light with the opposite handness will see the constant index of refraction $n = (n_e + n_o)/2$. It will be almost completely transmitted and Bragg reflection will occur[10] for $\lambda_0 = np$.

For our calculations, we choose for the birefringence of the LC $\Delta n = 0.23$. The mean value of the refractive index is $n = (n_e + n_o)/2 = 1.64$. These values correspond to the LC mixture E48 from Merck, which we use for our experiments. If other values are used, it will be mentioned. All calculations are done for circular polarized light that is incident parallel to the helical axis and has the same handness as the CLC. Its wavelength spectrum corresponds to the radiation of a blackbody with a surface temperature of 6000 K. The LC is sandwiched between glass plates with an index of refraction of $n = 1.5$. The thickness of the CLC layer is 10 μm.
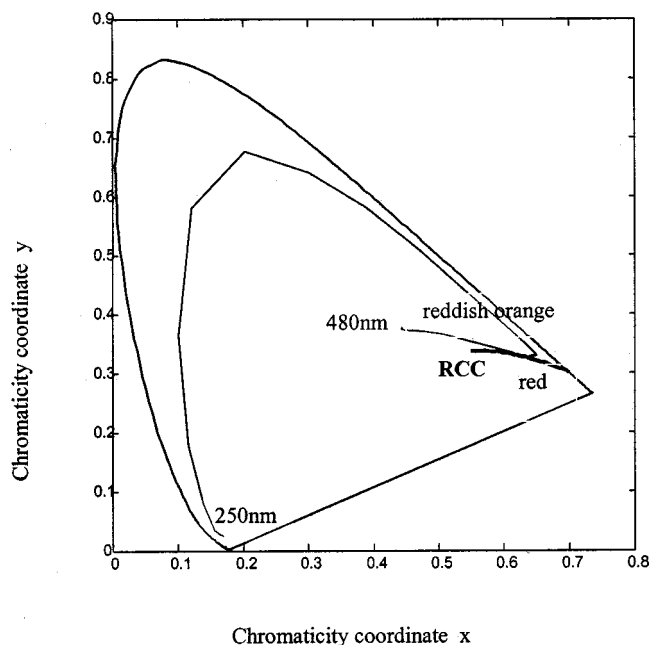
Fig. 1 Color coordinates in the chromaticity diagram CIE1931 for reflection spectra of a CLC with different pitches starting from 250 to 480 nm with an increment of 10 nm.

4 Orange Shift of Red CLCs

Before discussing the orange shift of red CLCs we introduce a definition for saturated red color as a function of the chromaticity coordinates x and y of the CIE1931 diagram. We call this the red color condition (RCC):

$$\text{RCC} = \frac{x^2 + y^2}{x - 0.17} \leq 1.095 \quad \text{for} \quad x \geq 0.55. \quad (3)$$

The formula for the RCC fits the border-line between reddish orange and red in the chromaticity diagram CIE1931 (see Fig. 1). Since the sum of x and y cannot exceed 1, the RCC is fulfilled automatically for all values of x greater than 0.7.
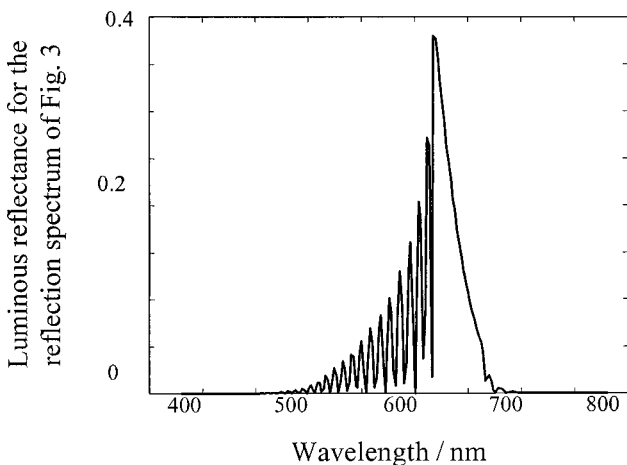
In Fig. 1, we present the calculated color coordinates of a 10-μm-thick CLC layer with pitches increasing from 250 to 480 nm in the CIE1931 chromaticity diagram. For short pitches, the color coordinates are in the blue area. With increasing pitch, they cross the green and yellow areas and they then turn—just before reaching the red region of the chromaticity diagram—to the white point ($x/y = 0.33/0.33$). The color coordinate x reaches a maximum of only 0.65 for a pitch of 390 nm. To analyze this behavior we calculate the reflection spectrum of a CLC with a pitch of 390 μm. The reflection spectrum shows strong side reflection bands next to the main reflection band (Fig. 2). These sidebands appear due to multiple interference on the CLC layer and scale with the value of the birefringence. For a red CLC layer, the sidebands on the short wavelengths side of the main reflection band have a great influence on the photometric property or rather physiological optical impression. The reflection spectrum of Fig. 2 is a radiometric spectrum. To evaluate chromaticity coordinates, we must consider the tristimulus values $x(\lambda)$, $y(\lambda)$,
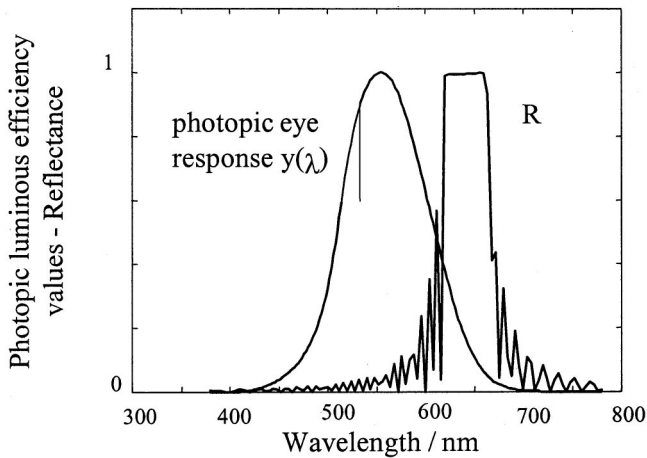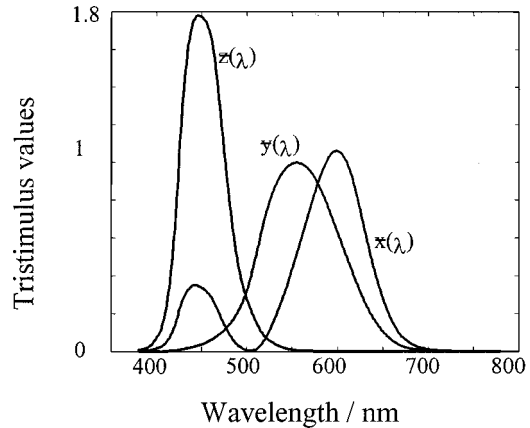
Fig. 2 Photopic eye response $y(\lambda)$ and the radiometric reflection spectrum R of a CLC with a pitch of 390 nm and a layer thickness of 10 μm. The side reflection bands are clearly seen.

Fig. 4 Color-matching functions of CIE1931 standard calorimetric observer $[z(\lambda), y(\lambda), x(\lambda)]$. The y curve is also known as the photopic spectral eye sensitivity, which has its maximum at 555 nm.

and $z(\lambda)$, as shown shortly in Fig. 4 and the spectrum of the light source. The "conversion" of the radiometric reflection spectra of Fig. 2 into a photometric one by multiplying it with the (photopic) spectral eye sensitivity, known as tristimulus curve "$y(\lambda)$" (Figs. 2 and 3), leads to an "amplification" of the side reflection bands for wavelengths shorter than $\lambda_0 = np$. Therefore the resulting color is orange rather than red.

To get a more general understanding of the problem, we considered also a blue CLC. If its radiometric reflection spectrum is multiplied with the photopic eye response, the result looks similar to the mirror image of Fig. 3 with the mirror plane at about 555 nm. Because of the weighting of the tristimulus curves (Fig. 4) and the fact that there is nearly no overlapping between $z(\lambda)$ and $y(\lambda)$, the perceived color is still pure blue (Fig. 1, the curve is just starting in the blue corner). In the case of the red color, there is a large overlapping between the $x(\lambda)$ and $y(\lambda)$ curves, and therefore the impact of $y(\lambda)$ on the red color stimuli is very important.

Fig. 3 Product of eye response and the reflection spectrum from Fig. 2.

We must add, of course, that due to the larger pitch of the red CLC, the reflected bandwidths of the main and sidebands are larger for the same Δn. Therefore the red color is less saturated compared with shorter pitch CLCs. Furthermore, the multidomain structure[11] of the cholesteric texture contributes also to the deterioration of the red color. In this structure the helical axis of the cholesteric domains are not all perpendicular to the substrate surfaces, and there is an angular distribution of the helical axis around the surface normal. The reflection spectrum of light incident perpendicular to the sample but oblique (at an angle θ) to the helical axis of a cholesteric domain, is shifted to shorter wavelengths corresponding to the condition for Bragg reflections:

$$\lambda = np \cos \theta. \qquad (4)$$

The reflection of light on an ensemble of domains results in a spectrum that is enlarged toward shorter wavelengths. In the case of blue CLCs the spectrum is enlarged toward the nonvisible UV, and the purity of the blue color is nearly unchanged and reflectance is maintained. In the case of red CLCs, the distribution of the helical axis produces an enlargement of the reflection spectrum toward orange increasing also the reflectance. As a result, the multidomain structure also contributes to the orange shift of the red CLC.

5 Improvement of Red Color Performance

To achieve pure red color with cholesteric LCDs, either the reflection sidebands described in Sec. 4 (Fig. 2) must be compensated or their occurrence must be prevented. In this section, on the basis of simulation results we discuss five alternative methods for improving the red color performance.

5.1 Filtering with Color Filters

The use of color filters is a well-known method for spectral filtering. The advantage of filters is that they have a sharp cutoff wavelength. Matched to the reflection spectrum of a red CLC, the superposition of an absorption filter and a red CLC should result in pure red color.
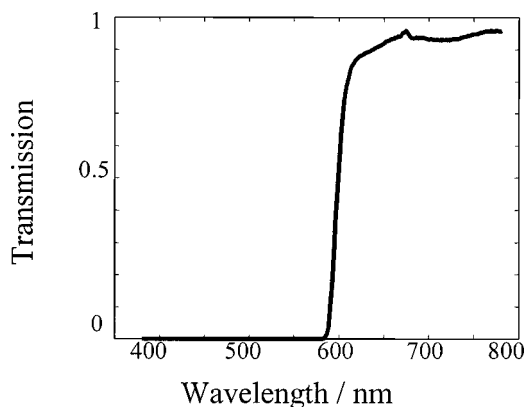
Fig. 5 Transmission spectrum of the Kodak w25 film.

For our simulations we used the transmission spectrum of an ordinary Kodak w25 film filter (Kodak SA, Lausanne, Switzerland), which was measured with the grating spectrophotometer Cary 1E (Varian Australia Pty. Ltd.). The filter has a cutoff wavelength of 590 nm (Fig. 5).

Figure 6 shows the calculated reflection spectrum of a CLC with an optimum pitch of 390 nm with and without superposition of the w25 film. Color filters normally also reduce the brightness, but the steep absorption edge of the filter at 590 nm limits the loss in reflection. Compared to Fig. 1 the reflection sidebands at shorter wavelengths are almost completely suppressed. The chromaticity coordinate x is greater than 0.7, which indicates pure red color. The RCC values for the filtered and nonfiltered CLCs are 1.089 and 1.100, respectively.

5.2 Filtering with Dichroic Dyes

By doping the CLC with a dichroic dye, its original colorimetric values can be altered.[7] The absorption of dichroic dyes is polarization dependent. Figure 7 shows the absorption spectra that were measured polarization dependent (parallel and perpendicular to the molecular alignment) on a test cell with planar and antiparallel alignment without twist. The cell is filled with a mixture of E48 doped with 1.0 wt% of the dye D35 from BDH Merck. The cell gap is
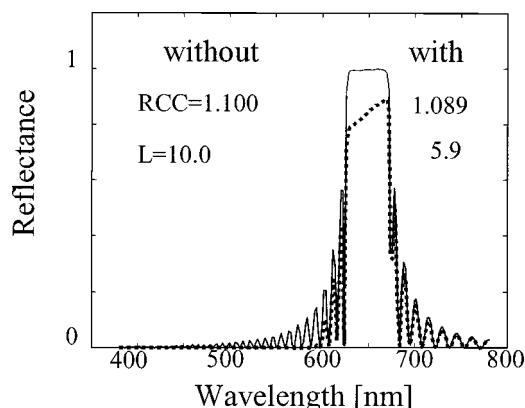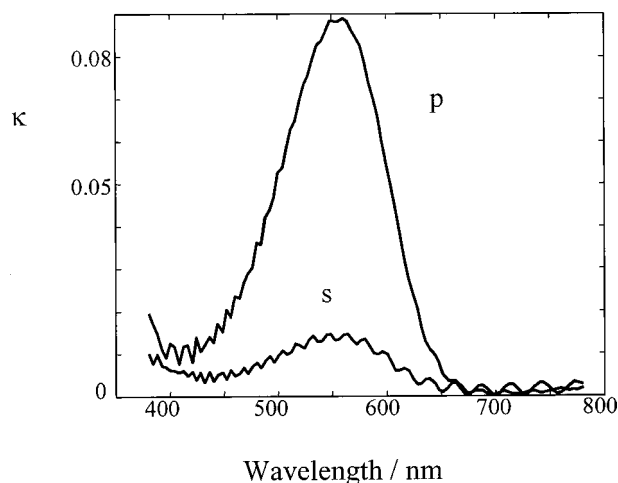

Fig. 7 Spectral absorption coefficient of an LC layer with 1 wt% D35. The two curves are related to the *s* and *p* polarizations.

6 μm. The spectral absorption coefficients $\kappa(\lambda)$ for parallel and perpendicular polarization were calculated by the Lambert-Beer law ($d =$ cell gap):

$$T(\lambda) = \exp[-\kappa(\lambda)d]. \tag{5}$$

Due to different penetration depths, there is no well-defined cutoff wavelength of the reflected light. The reflected light at upper layers in the CLC is not complete absorbed. The color of this dye-doped LC is less saturated than that obtained with spectral filtering by filters. The brightness is higher than in the case of filtering with film filters in front of the CLC layer. Figure 8 shows the calculated reflection spectrum of a dye-doped CLC. The RCC value for our parameter set is 1.090.

5.3 Small Birefringence CLC

A small birefringence Δn causes a narrow reflection band $\Delta\lambda$ according to the relation $\Delta\lambda = \Delta np$, where p is the length of the pitch. Figure 9 shows a typical reflection spectrum for a CLC with $\Delta n = 0.07$. The amplitude and band-
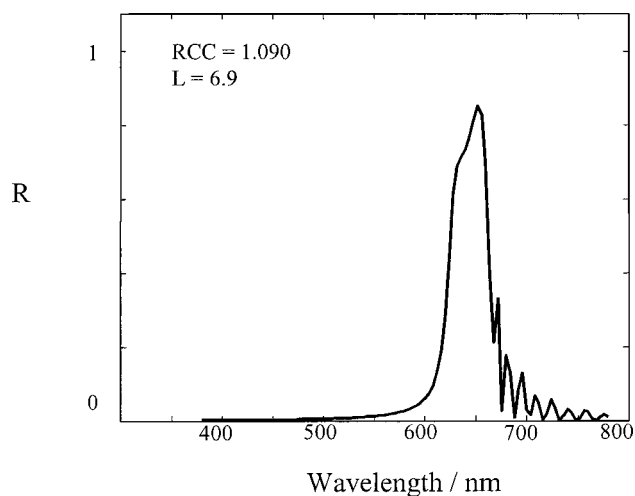

Fig. 6 Comparison of the reflection spectra with (dashed line) and without (solid line) filtering, *L* is the luminous reflectance.

Fig. 8 Reflection spectrum of a dye-doped CLC (pitch, 390 nm).
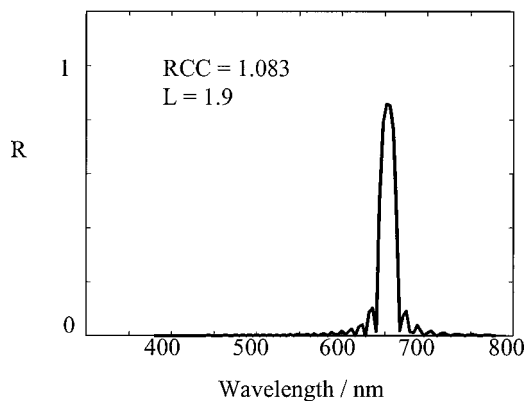
Fig. 9 Reflection spectra of a CLC with $\Delta n = 0.07$ (pitch, 400 nm).

Fig. 11 Reflection spectrum generated by the index profile shown in Fig. 10. The pitch of the CLC is 400 nm.

width of the side reflection bands are reduced, but even with this small Δn value, the sidebands are not removed. The red color condition, however, is fulfilled and the RCC value is 1.083. The luminous reflectance is strongly reduced because of the small main reflection bandwidth.

5.4 *Birefringence Depth Profile in CLC*

A depth profile of the birefringence perpendicular to the LC layer is approximated by thin layers in which the birefringence is constant (see Fig. 10). From layer to layer, the birefringence decreases linearly. The birefringence Δn starts at 0.23 and is decreased by 0.023 for every micrometer. As we can see in Fig. 11, the sidebands are almost eliminated. Nearly no yellow light can deteriorate the pureness of the red light that is reflected from the main reflection band. The RCC value is 1.092 and slightly below the limit 1.095.

Other depth profiles of the birefringence than that of Fig. 10 can also produce color purifications. The effect of different types of linear and nonlinear profiles in CLCs are described elsewhere.[12]

5.5 *Additive Color Mixing*

In this method, we added a blue reflector behind the red-orange CLC layer. A blue CLC can also be used as the blue reflector. In our simulation, we consider a double cell of a
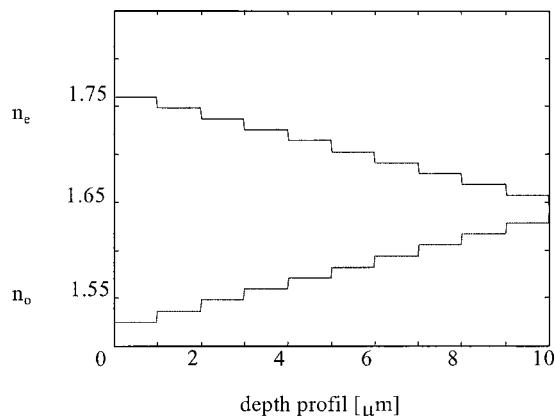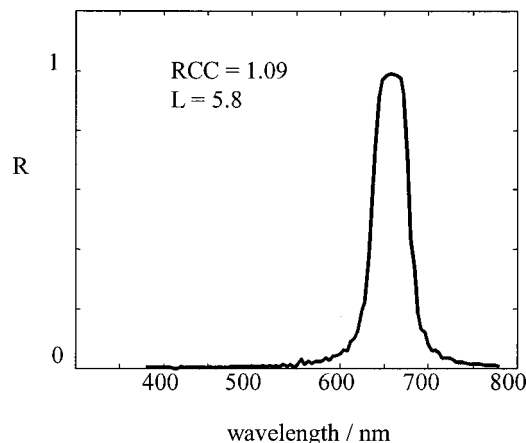
red CLC on top of a blue CLC, the pitches being 395 and 265 nm. This configuration enables us to easily vary the amount of reflected blue light by varying the thickness of the blue CLC. The resulting color of such a stack is determined by the ratio of the thickness of both layers. In Fig. 12, the trace of the chromaticity coordinates in the CIE1931 standard observer diagram is shown as a function of the thickness ratio. This trace is almost a straight line between the color points for the single layers. Only a thin blue layer is required to fulfil the red color condition for the stack. The required thickness of the blue CLC layer is between 1 and 3% of that of the complete CLC stack. The resulting red color is not very saturated but it is quite bright. The RCC value is 1.054 for the selected parameter set. Figure 13 presents the reflection spectrum of the double layer.

6 Experimental Results

The nematic host for our experimental LC mixtures was E48 from Merck (Merck KGaA, Darmstadt, Germany). To

Fig. 10 Profile of the ordinary and extraordinary indices in a CLC layer with 10 μm thickness.
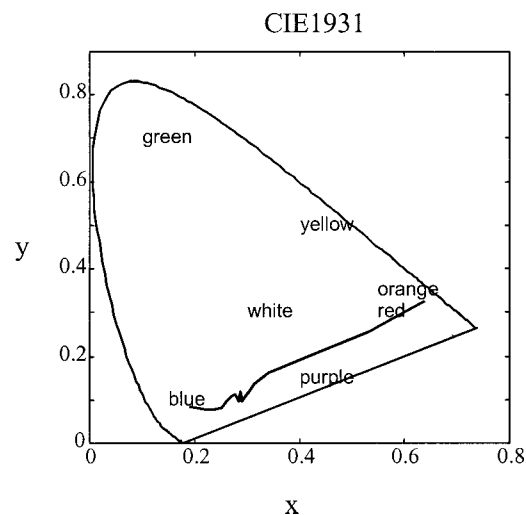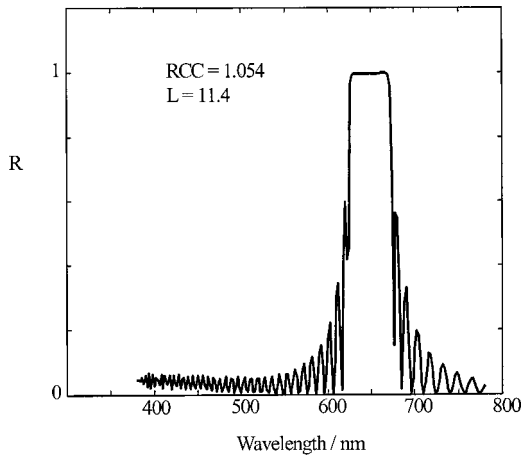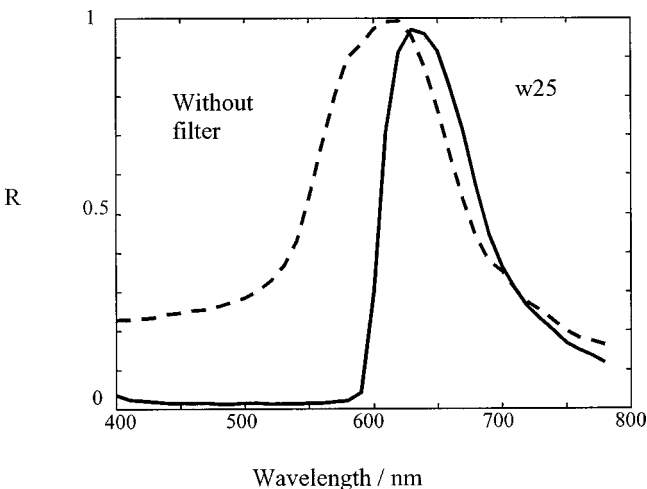

Fig. 12 Color trace of the double layer with pitches of 265 and 395 nm starting in the reddish orange (pitch, 395 nm) and ending in the purplish blue (pitch, 265 nm).
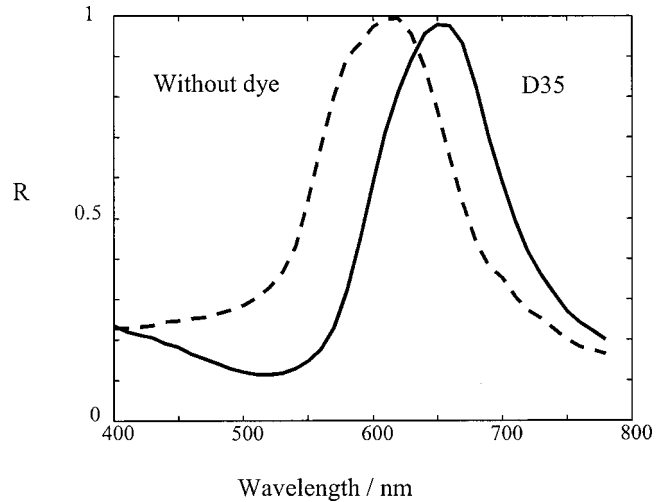
Fig. 13 Reflection spectrum of the double layer with the pitches 265 and 395 nm, the blue layer being 2% of the total thickness of the CLC stack.

Fig. 15 Reflection spectra of a CLC without (dashed line) and with (solid line) filtering with the D35 dye.

adjust the cholesteric pitch we used three commercially available nonmesogenic chiral dopants of the same handness. All of our test mixtures are used without a stabilization of the cholesteric texture by polymers. The inner surfaces of our test cells are treated with nonrubbed commercially available polyimide. The polyimide induces planar alignment. The nominal cell gap is 6.0 μm. The colorimetric measurements of the multidomain CLC structure are made in the reflection mode with the "λ-scan" module of a display measuring system (DMS) from Autronic-Melchors (Autronic GmbH, Karlsruhe, Germany). The samples are illuminated with diffuse light and the detecting optic is tilted to 3 deg from the normal. The geometry of our illumination systems eliminates specular reflections from the surface of the LC cell. We use a white standard from Labsphere to define the reflectance of 100%. The indicated colorimetric values are calculated for a standard D65 illuminant. All of the shown reflection spectra are normalized to 1.

6.1 Filtering with Color Filters

Figure 14 shows the reflective spectra for the nonfiltered and filtered cells. To measure the reflection spectrum of our red CLC with the color filter film from Kodak (type w25, transmission spectrum in Fig. 5) we simply put the filter on top of our test cell. Since specular reflections are eliminated by the measurement geometry, we are not concerned about Fresnel reflections on the glass surfaces. The matching of the CLC and the filter are not optimized, therefore the filter also cuts some red light. This partial misfit explains the poor reflectance of only 5.0%. The RCC value for the filtered spectrum is 1.083, whereas, for the nonfiltered sample, the chromaticity coordinate x is smaller than 0.55, which means that the RCC is not applicable.

6.2 Filtering with Dichroic Dyes

To study the influence of dyes we doped our red CLC mixture with 0.5 wt% of the dichroic dye D35 from BDH Merck (Merck Ltd., Merck House, Poole, Great Britain).

Fig. 14 Reflection spectra of a CLC device without (dashed line) and with (solid line) filtering with the Kodak w25 filter.

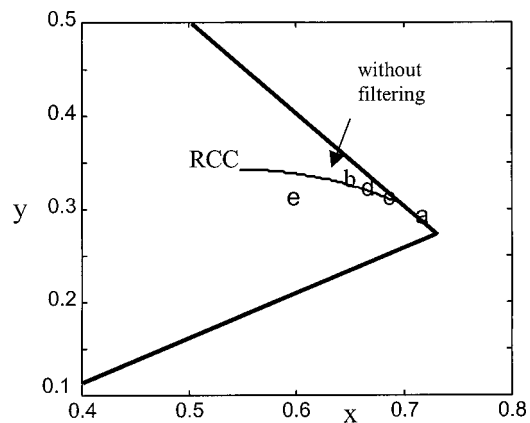**Fig. 16** Chromaticity coordinates for the different methods: e represents the less-saturated red, whereas a is the solution with the purest red: a, filtering with color filters; b, filtering with dyes; c, small birefringence; d, birefringence depth profile; and e, additive color mixing.

Table 1 Comparison (theory) of the different methods to generate red color.

Method*		x	y	RCC	Reflectance (%)
Red CLC	0	0.64	0.33	1.100	10.5
Red CLC with color filter, Kodak w25	a	0.71	0.29	1.089	5.4
Red CLC with dye, 1 wt% D35	b	0.65	0.32	1.090	7.2
Red CLC with $\Delta n = 0.12$	c	0.68	0.31	1.089	4.6
Red CLC with Δn—gradient	d	0.66	0.32	1.092	5.8
Red CLC with blue reflector ($d_{reflector}/d_{total}=0.02$)	e	0.59	0.31	1.054	11.4

*Note method letters refer to Fig. 16.

The absorption spectra of this dichroic dye in a nematic LC is shown in Fig. 7. The reflection spectra of the nondoped CLC and of the dye-doped CLC are presented in Fig. 15. The reflectance at lower wavelengths is not completely measured. The RCC is even not applicable for the reflection spectrum of the dye doped CLC mixture because the chromaticity coordinate x is smaller than 0.55.

7 Discussion

Each of the five possibilities presented leads to an improvement of the purity of the red color but all of them—with the exception of the method Sec. 5.5—considerably reduce the reflectance. Figure 16 shows the location of the chromaticity coordinates for the different methods in the CIE1931 diagram. The arrow points onto the original CLC. We can see that filtering with a matched color filter yields the most-saturated red and the use of a blue reflector behind the red CLC results in a less-saturated red. However, brightness is best for the method that gives the less-saturated red—instead of absorbing orange light we are adding blue light—and worst for the method giving the purest red. In display applications, a trade-off must be made between brightness and color performance. The numerical results are shown in Table 1.

The results of our experiments are compared in Table 2, and Fig. 17 shows the location of the chromaticity coordinates in the CIE1931 diagram. The test cell with a red CLC mixture (peak reflection wavelength 620 nm) looks orange and the color coordinates are located close to the white point. Making the pitch bigger does not solve the problem. The cells just look "dirty red" and the brightness is reduced. Adding the film color filter from Kodak on top of the cell clearly gives the best red color performance, but unfortunately the reflectance is strongly reduced compared to the original red CLC (Table 2). A better match of the CLC mixture and the filter should result in a reasonable compromise for display applications. The improvement of the red color with a dye-doped mixture is far from being as good as for the method using a filter but it still is signifi-

cant. The reduction of the brightness is reasonable for the gain of color saturation. An optimization of the dye-doped CLC should give much better results as presented here.

We believe that only the methods with spectral filtering and the method using an additional blue reflector behind the red CLC can be applied for displays applications. The easiest approach would be to dope the CLC with dyes, because this will not interfere with the cell technology. A drawback could be the chemical instability of these dyes. This instability can create problems for the lifetime of displays, especially in outdoor use. Adding a color filter in front of the CLC layer would give better results for color saturation (method a in Table 1) but is—at least for micro-color filters—interfering in an important way with the manufacturing process and costs. A display based on small-birefringence mixtures is not useful due to its low brightness. The use of a gradient of birefringence parallel to the helical axis would be an interesting approach for the realization of red color filters with good color performance, but the implementation of such a gradient in a CLC cell is not obvious.

A comparison of our theoretical and experimental results is difficult. There are many differences between the assumed theoretical model and the real LCD. The theoretical model is based on a perfect Grandjean texture[13] with its helical axis perpendicular to the cell normal and a collimated illumination parallel to the helical axis. The light reflection is analyzed only parallel to the helical axis. However, in a real LCD based on the cholesteric texture, the planar reflective state has a multidomain structure with a certain distribution of the helical axes around the cell normal and there a pitch distribution also occurs.[11] Both the helical axis and the pitch distribution enlarge the reflection band of the red CLC, which gives less-saturated red color. The multidomain structure also causes some scattering to appear. Last but not least, a display is normally viewed at a certain viewing angle with more or less diffuse ambient illumination.

Table 2 Comparison (experimental) of the different methods to generate red colored CLC.

Method*		x	y	RCC	Reflectance (%)
Red CLC	f	0.44	0.38	na	21
Red CLC with color filter (Kodak w25)	g	0.65	0.31	1.083	5.0
Red CLC with dye, 0.5 wt% D35	h	0.47	0.34	na	15

*Note method letters refer to Fig. 17.
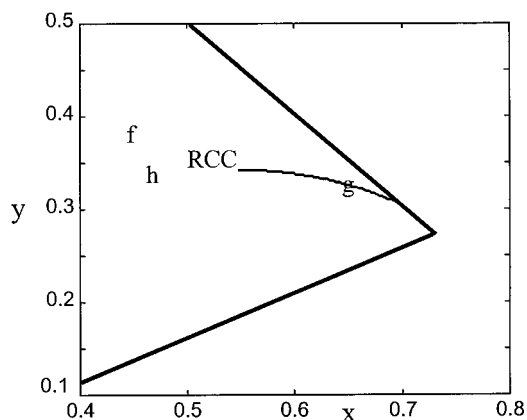
Fig. 17 Comparison of the experimental solutions: f, no filtering; g, Kodak filter; and h, dye.

We undertook the theoretical work to qualitatively understand the red color problem. The experimental work was done to get a quick check of the possibilities with color filters and dyes. For the experiments, we used materials that were readily available. Further work is still required to evaluate and to optimize these approaches in view of display applications.

8 Conclusion

The poor red color performance of red CLCs was analyzed theoretically. We introduced therefore a formula, the RCC. We found five possible concepts to improve this performance on the basis of theoretical simulations. Experimentally, we demonstrated the red color performance of CLC displays for two of these concepts. They are based on spectral filtering, which absorbs the light in the sidelobes situated in the yellow and orange regions. The birefringence gradient method seems to be technologically very demanding and in addition its long-term stability due to diffusion of dopants is undetermined. The additive color mixing method does not suppress the sidelobes and therefore yields the brightest but less saturated red.

The choice of the method depends on its application.

References

1. A. Sato, "Reflection formats for color LCDs solve power-consumption problems," in *Display Devices* **10**, pp. 18–21 (1994).
2. Y. Itoh, N. Kimura, Y. Ishii, F. Funada, and K. Awane, "Development of 512-color-reflective TFT-LCD," in *IDW '96, Proc. 3rd Int. Display Workshops*, Vol. 1, pp. 409–412, Inst. of Television Engineers of Japan and Soc. Info. Display, Japan Chapter, Kobe, Japan (1996).
3. T. Ishinabe, T. Uchida, M. Suzuki, and K. Saito, "A bright full color reflective LCD using optically compensated bend cell (R-OCB cell) with fast response," in *SID EuroDisplay, Proc. 16th Int. Display Research Conference*, pp. 119–122, Soc. of Info. Display, Birmingham, England (1996).
4. D. Davis, A. Kahn, X. Y. Huang, J. W. Doane, and C. Jones, "Eight-color high-resolution reflective cholesteric LCDs," in *SID Int. Symp., Digest of Technical Papers*, Vol. XXIX, pp. 901–904, Soc. of Info. Display, Anaheim, California (1998).
5. K. Hashimoto, M. Okada, N. Nishiguchi, N. Masazumi, E. Yamakawa, and T. Taniguchi, "Reflective color display using cholesteric liquid crystals," in *SID Int. Symp.*, Digest of Technical Papers, Vol. XXIX, pp. 897–900, Soc. of Info. Display, Anaheim, CA (1998).
6. L.-C. Chien, U. Müller, M.-F. Nabor, and J. W. Doane, "Multicolor reflective cholesteric displays," in *SID Int. Symp., Digest of Technical Papers*, Vol. XXVI, pp. 169–171, Soc. of Info. Display, Orlando, FL (1995).
7. J. L. West, "The challenge of new applications to liquid crystal displays," in *Liquid Crystals in Complex Geometries formed by Polymer and Porous Networks*, G. P. Crawford and S. Zumer, Eds., pp. 255–264, Taylor and Francis, London (1996).
8. D. M. Makow and M. David, "Peak reflectance and color gamut of superimposed left- and right-handed cholesteric liquid crystals," *Appl. Opt.* **19**, 1274–1277 (1980).
9. M. G. Moharam, D. A. Pommet, E. B. Grann, and T. K. Gaylord, "Stable implementation of the rigorous coupled-wave analysis for surface-relief gratings: enhanced transmittance matrix approach," *J. Opt. Soc. Am. A* **12**, 1077–1086 (1995).
10. D. M. Makow, "Color properties of liquid crystals and their applications to visual arts," *Color Res. Appl.* **4**(1), 25–32 (1979).
11. W. D. St. John, W. J. Fritz, Z. J. Lu, and D.-K. Yang, *Phys. Rev. E* **51**, 1191 (1995).
12. J. Grupp, P. Kipfer, T. Scharf, C. Bohley, R. Klappert, and H. P. Herzig, "Dispositif optique *à* réflexion de Bragg et procédés pour sa fabrication," European Patent application No. 99115390.9 (1999).
13. F. Grandjean, "Existence de plans differenciés équidistants normaux à l'axe optique dans les liquides anisotrope," *Compt. rend.* **172**, 71 (1921).

Peter Kipfer studied physics in Erlangen, where he received his Diploma in 1989. In 1995 he finished his thesis about artificial dielectrics with the Chair of Optics, University Erlangen, Germany, in the group of J. Schwider. From 1996 to 2000 he was post-doc with the Institute of Microtechnology in Neuchâtel, Switzerland, in the group of Dändliker and Herzig. His activities are optical design of micro-optical elements.

Rolf Klappert received a degree in physics from Münster University, Germany, in 1986. He has been working in the field of liquid crystal research since 1984 and joined the display group of ASULAB S.A., Switzerland, in 1987. ASULAB is the R&D facility of the Swatch Group. He currently works as a project manager and is a member of the SID and the ILCS.
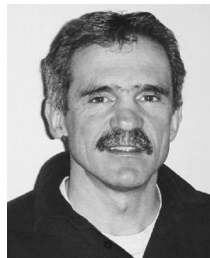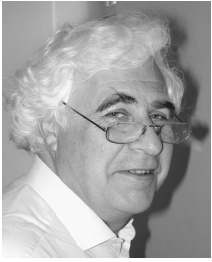
Hans Peter Herzig received his diploma in physics from the Swiss Federal Institute of Technology, Zürich, in 1978. From 1978 to 1982 he was a scientist with the Optics Development Department of Kern in Aarau, Switzerland, working in lens design and optical testing. In 1983, he became a graduate research assistant with the Applied Optics Group at the Institute of Microtechnology of the University of Neuchâtel, Switzerland, working in the field of holographic optical elements, especially scanning elements. In 1987, he received his PhD degree in optics. He currently heads the micro-optics research group and is a professor at the University of Neuchâtel. Dr. Herzig is member of OSA and EOS and a board member of the Swiss Society of Optics and Microscopy.
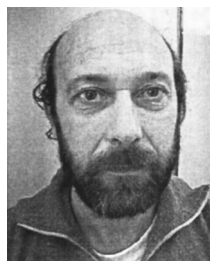
Joachim Grupp received his degree in physics from the Physics Institute of the Westfälische Wilhelms-Universität, Münster, Germany, in 1976. After obtaining his PhD in science in 1982, he was a senior scientist in the field of liquid crystals at the Physics Institute in Münster. He joined ASULAB in 1984 as project leader for liquid crystal matrix displays. He became head of the Group in 1987 and is the inventor or coinventor of more than 30 patents in the field of electro-optical systems, liquid crystal displays, and micro-electronics. He is member of DPG, SID, SPIE, and DGAO.

René Dändliker received his diploma in physics from the Swiss Federal Institute of Technology, Zürich, in 1963, his PhD in physics from the University of Berne, Switzerland, in 1968, and the Venia Legendi for applied physics from the Swiss Federal Institute of Technology, Zürich, in 1978. From 1963 to 1969 he was a graduate research assistant with the Institute of Applied Physics, University of Berne, working on gas and solid-state lasers. From 1969 to 1970 he was a research scientist with the Philips Research Laboratories, Eindhoven, Netherlands, working in the field of applied optics. From 1970 to 1978 he was a senior scientist and head of the Coherent Optics Group at the Brown Boveri Research Center, Baden, Switzerland, where he was concerned with optical metrology applied to mechanics, such as laser Doppler velocimetry and heterodyne holographic interferometry. Since 1978 he has been a professor of applied optics with the University of Neuchâtel, Switzerland, and since 1989 also a professor of applied optics with the Swiss Federal Institute of Technology, Lausanne. His current research activities are in optical metrology, optical fibers and sensors, holography and optical computing, diffractive optical elements, and micro-optics. Dr. Dändliker was president of the European Optical Society from 1994 to 1996, and he is a vice president of the International Commission for Optics, a fellow of the OSA and the Swiss Academy of Engineering Sciences, an honorary member of the Swiss Society of Optics and Microscopy, a member of the SPIE, the French Society of Optics, the Germany Society of Applied Optics, and the European Physical Society, and an affiliate of LEOS/IEEE.